Journal of The Electrochemical Society, **153** (9) B337-B343 (2006)
0013-4651/2006/153(9)/B337/7/$20.00 © The Electrochemical Society

Copper Repassivation Characteristics in Carbonate-Based Solutions

Esta Abelev,[a,*] Andrew Jonathan Smith,[b] Achim Walter Hassel,[b,] and Yair Ein-Eli[a,**,z]**

[a]*Department of Materials Engineering, Technion-Israel Institute of Technology, Haifa 32000, Israel*
[b]*Max-Planck-Institut für Eisenforschung, D-40237 Düsseldorf, Germany*

The present work reports on carbonate-based solutions, which can provide copper passivity in a wide potential range. This report focuses mainly on the identification of copper repassivation features obtained subsequent to mechanical damage of copper passive films in carbonate-based solutions. The repassivation rate of copper in carbonate-based solutions was measured with the use of a slurryjet system. The measured repassivation rate of copper in a slurryjet system utilizing a carbonate-based solution was found to be in the range of 1–2 ms. An increase in the concentration of carbonate ions leads to a decrease of the copper repassivation time at potentials ranging from 200 to 600 $mV_{Ag/AgCl}$. The impingement angle between the copper surface and the single abrasive particle has an insignificant impact on the repassivation time and characteristics. It is therefore recommended that the use of carbonate anions as a passivating component in a future chemical mechanical planarization slurry design should be considered.
 [DOI: 10.1149/1.2213547]

Manuscript submitted March 6, 2006; revised manuscript received April 11, 2006. Available electronically June 29, 2006.

The interest in the electrochemical behavior of copper in various electrolyte systems has significantly increased in the last decade, due to the role of copper in the microelectronic industry.[1] Copper is currently recognized as the sole replacement for aluminum in integrated circuit (IC) interconnects. Copper dual damascene technology includes two electrochemical steps: electroplating and chemical mechanical planarization (CMP).[1] The main purpose of CMP application is to remove copper overfilling from interconnects patterning through a rapid dissolution, leading to a global planarizing of the wafer surface.[1-6]. In order to optimize the copper CMP process, various chemicals, abrasives, and polishing pads have been suggested throughout the past years.[1-13] However, effective CMP can only be envisioned in solutions where metals and in particular, copper, are characterized with certain electrochemical characteristics: selfpassivation in the CMP slurry, fast dissolution of exposed surface sites activated by direct contact with the pad and abrasive, and finally, a rapid repassivation of the activated and exposed sites during further exposure. Thus, the necessary feature expected of the copper CMP slurry is to provide a rapid repassivation of the metals to be planarized.[6,7,14]

Copper CMP slurry designers should consider the potential-pH plot (Pourbaix diagram), which predicts copper passivity in a pH region between 7 and 13, i.e., in neutral and alkaline solutions.[15] Therefore, copper passivity and an efficient CMP process obviously cannot be realized in acidic solutions. Thermodynamic calculations indicate that copper passivity in aqueous solutions can be achieved in a pH range of 7–13 and at potentials above 0.461–0.0592 (pH) V_{SHE}.[15] The oxides covering the copper surface in this region are mainly Cu_2O, CuO, and $Cu(OH)_2$.[16-25]

In addition to the crucial impact of the pH, copper passivity can be strongly affected with the introduction of various anions into the solution. It is known that while certain anions can reduce the protective characteristic of the passive film either by initiating a breakdown of the passivity or by forming an insoluble nonprotective salt, other anions can stabilize the passivity.[26]

The electrochemical behavior of copper in carbonate-containing solutions was already reported in a wide pH range, from slightly acidic to alkaline solutions.[19,21,27-31] It was reported that in alkaline solutions containing $NaHCO_3$ and Na_2CO_3 a protective anodic film is formed.[32] This film is composed of an inner Cu_2O film and an outer $CuO/Cu(OH)_2$–$CuCO_3$ complex layer. Likewise, a stable form of copper surface film was formed in alkaline solutions containing Na_2CO_3 having pH values above 10. The film consisted of Cu_2O, CuO, and different complex anionic species containing copper carbonates $\{CuCO_3{\cdot}Cu(OH)_2$, $2CuCO_3{\cdot}Cu(OH)_2$, and $[CuCO_3(OH)_2]^{-2}\}$.[19] Tromans and Sun[20] studied the anodic behavior of copper in weak alkaline solutions (pH values of 9.4–10.8) containing 1.0 M sodium sulfate and an addition of a buffer (bicarbonate/carbonate, HCO_3^-/CO_3^{2-}). They suggested that sulfate ion adsorption on the oxidized copper surface is the important factor in film breakdown. Mattsson and Fredriksson[33] indicated that pitting is likely to be avoided if the pH value is above 7 and the solution consists of HCO_3^- ions. These conditions stimulate the formation of a protective film composed of basic copper carbonate salts, $CuCO_3{\cdot}Cu(OH)_2$, or azurite, $2CuCO_3{\cdot}Cu(OH)_2$, formed at the copper surface.[33] Thomas and Tiller[34] studied copper behavior in neutral solutions containing HCO_3^-. They reported that bicarbonate (HCO_3^-) ions in a concentration of 0.01 M could promote pitting corrosion attack of copper in neutral solutions. An increase in the HCO_3^- concentration to 0.1 and 0.5 M reduces the protective characteristics of copper-oxide film, most probably due to the increase in soluble copper carbonate complexes formation.

Therefore, the study of the electrochemical behavior of copper in basic solutions is essential, because up-to-date, copper passivity in a wide potential range with the capability of producing protective characteristics is not fully implemented in current CMP processes. This report is focused on the identification of the copper passivity parameters: potential range, repassivation, and depassivation time of copper in carbonate-based solutions. It is the first time that the repassivation rate of copper in carbonate-based solutions is being reported.

Experimental

Electrochemical experiments.— A pencil-type electrode made of 5 mm diameter copper rod (99.9995 wt %) mounted in a room-temperature-curing epoxy was used in the electrochemical measurements. After polishing to 1200 grit SiC paper, the samples were carefully degreased with acetone and rinsed with double-distilled water. The electrochemical measurements were conducted with a 273A EG&G potentiostat (Princeton Applied Research) in a 500 mL three-electrode electrochemical cell equipped with a Ag/AgCl reference electrode connected through a salt bridge and a Pt counter electrode. The reference electrode was installed in the solution through a Luggin–Haber capillary tip assembly. All the potentiodynamic experiments and cyclic voltammetry were scanned at 1 mV/s.

* Electrochemical Society Student Member.
** Electrochemical Society Active Member.
z E-mail: eineli@tx.technion.ac.il

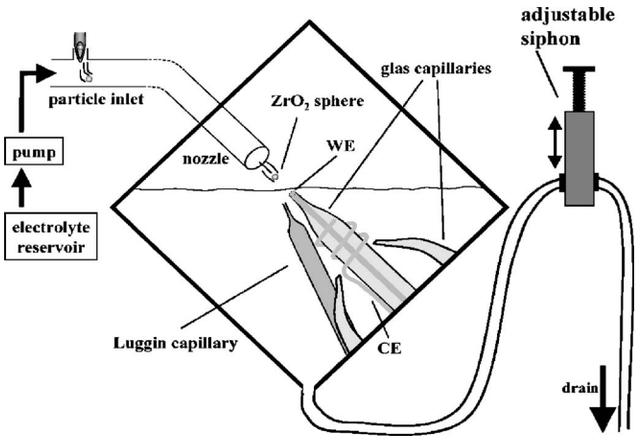

Figure 1. Schematic of the SlurryJet impingement system. The slurry ejecting nozzle faces the immersed working electrode (WE) and can be adjusted by an x-y-stage. The counter and reference electrode are in close vicinity to the WE. The adjustable siphon allows precise control of the electrolyte level in the chamber, taken from Ref. 35.

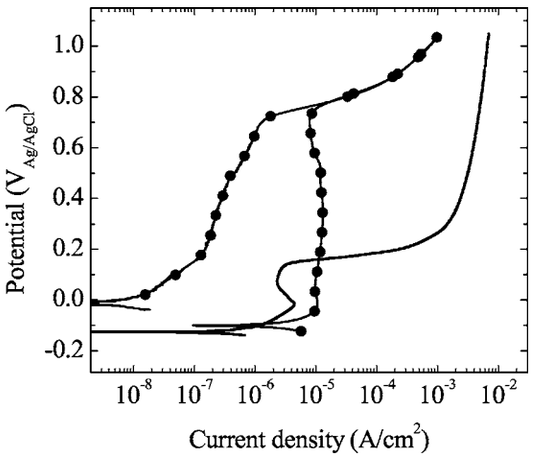

Figure 2. Potentiodynamic curves obtained from polarizing copper (–) in carbonate-free solution containing 1 g/L Na_2SO_4 and (●) in a solution containing both sulfate and 4 g/L K_2CO_3 (pH 11). pH of the carbonate-free solution containing sulfate ions was adjusted to 11 by adding KOH.

Chemicals.— Solutions were prepared with deionized water (DI, 18 MΩ cm, Millipore system) with the addition of analytical grade chemicals, such as K_2CO_3 and Na_2SO_4. All chemicals were purchased from Aldrich Chemicals.

Slurryjet instrument.— Copper repassivation rate in carbonate-based solutions was studied in a slurryjet impingement system which was developed at the Max-Planck-Institut für Eisenforschung, Düsseldorf, Germany.[35]

Electrodes.— High-purity copper 99.999% wire (Goodfellow, diameter 125 μm) was used in the preparation of miscrodisk electrodes. Glass capillaries were produced by means of a capillary puller (Narishige) and ground to a diameter of 140 μm. Subsequent to inserting the wire to the capillary, room-temperature-curing epoxy was drawn into the capillary using a vacuum pump. After epoxy hardening the microelectrode was mounted in a mechanically stable second glass capillary (made of a Pasteur pipette). The counter electrodes consisted of Au wires (99.999% Wieland Dentaltechnik) with a diameter of 200 μm which were wrapped around the capillary in the shape of a spiral. A Ag/AgCl reference electrode was connected via a Luggin capillary (Fig. 1) in all slurryjet studies. Figure 1 presents the schematic view of the slurryjet system. A detailed description of the slurryjet system can be found in Ref. 35 and 36.

Prior to each experiment the μ-electrodes were ground by a 3 μm diamond disk. Different impingement geometries were realized by grinding the samples at different angles. Afterwards, in order to decrease surface roughness, the μ-electrodes were electrochemically polished using the following solution: 1200 g/L H_3PO_4 with 120 g/L CrO_3 (density of solution was 1.71 kg/L) for 10 s at 2 V.

Slurry jet.— The slurry jet consists of an acrylic, cube-shaped chamber set on a corner (Fig. 1). The nozzle (made from a Pasteur pipette, 1 mm diameter) and the sample are mounted to facing walls of the chamber. A high-performance pump with an extreme acceleration of 20,000 revolutions s^{-2} reaches its maximum speed within 3 ms, in order to allow instant spraying. The lower tip of the cube acts as a drain. By mounting the nozzle to an x-y-stage it was possible to aim the electrolyte/slurry flow at the sample. By applying an adjustable siphon to the drain the electrolyte level in the chamber can be precisely adjusted (Fig. 1). In order to introduce a well-defined number of spheres into the system, a particle inlet was constructed from Plexiglas with a main channel for the electrolyte and a small perpendicular loading channel through which the spheres were introduced to the system using a hypodermic needle. Neither electrolyte nor impacting particles were recycled.[35]

Abrasive particles.— The abrasive particles used in these experiments were made of zirconia spheres (Fuji, Japan) with a mean size of 117 μm; the 2σ range (68%) ranged between 112 and 122 μm. The diameter of the electrode is almost identical to that of the particles. Thus, it was impossible for two particles to hit the surface simultaneously.[35]

Electronics.— A crucial point in the measurement of current transients during slurry jet impingement is the data acquisition because it contains important information about the repassivation mechanism.[35] Because the impact time of the particle is not exactly known but the transient of interest should be recorded with a sufficient resolution, it is desirable to use a high data acquisition rate. Further explanations regarding the electronics of the system can be found in Ref. 35.

Results and Discussion

Potentiodynamic measurements.— Figure 2 presents anodic potentiodynamic curves obtained from copper polarization in 1 g/L Na_2SO_4 carbonate-free solution and with the addition of 4 g/L K_2CO_3. Both of the solutions had a pH value of 11, while the carbonate-free solution containing only 1 g/L Na_2SO_4 was buffered with KOH. A positive potential sweep was applied from a potential slightly below the open-circuit potential (OCP). In a solution containing both 1 g/L Na_2SO_4 and 4 g/L K_2CO_3, the potentiodynamic scan was reversed when the anodic current density reached a value of 1 mA/cm^2. A small anodic current peak was detected at a potential of -0.015 $V_{Ag/AgCl}$ in a 1 g/L Na_2SO_4 carbonate-free solution (pH 11 buffered by KOH). During a further positive potential scan, the anodic currents gradually increased, indicating an active copper dissolution. The addition of 4 g/L potassium carbonate to 1 g/L Na_2SO_4 solution significantly affects the electrochemical behavior of copper. A small anodic current peak and a wide region of copper passivity up to 0.7 $V_{Ag/AgCl}$ can be seen in the anodic curve obtained from the positive potential scan. A rapid increase in anodic currents at a potential above 0.7 $V_{Ag/AgCl}$ was obtained up to a value of 1 mA/cm^2. Once the scan was reversed at potential of 1 $V_{Ag/AgCl}$ (at this potential the anodic current density was equivalent to 1 mA/cm^2) the anodic currents decreased, indicating that the copper substrate maintains its protective layer, formed during the positive anodic scan and thus remained in a passive state. The observed

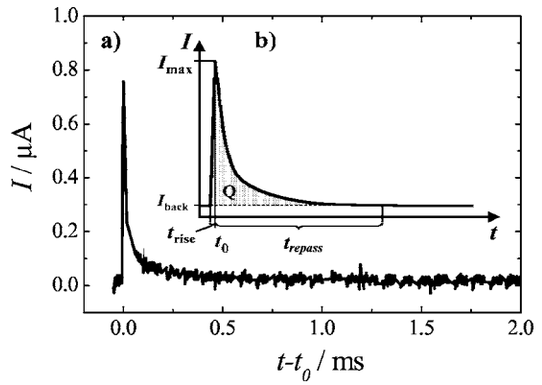

Figure 3. (a) Current transient normalized to the time of peak current, t_0, and (b) schematic current transient with marked characteristic sections. Studies were performed at applied potential of 0.2 $V_{Ag/AgCl}$ in a 4 g/L K_2CO_3 solution containing 1 g/L Na_2SO_4 solution.

increase in the anodic current at a potential above 0.7 $V_{Ag/AgCl}$ is attributed to oxygen evolution. Therefore, one can easily see that the copper passivity range was significantly affected by the addition of carbonate anions to the sulfate solution.

Repassivation time measurements.— As was mentioned above, one of the main requirements in the CMP process is a high repassivation rate of the metal which is being polished. The initial and promising electrochemical results reported elsewhere stimulated the study of the repassivation rate of copper in carbonate-based solutions.[31] This study of copper repassivation rate was performed with the use of a slurryjet system.

A copper microelectrode with a diameter of 125 μm was mounted from the lower side into the cube cell, as shown in Fig. 1. The cell siphon was adjusted in a way that the electrolyte covering the metal electrode of interest allowed potentiostatic control of the sample while minimizing the retardation of the jet once it entered the solution.

A copper microelectrode was polarized potentiostatically ($V_{constant}$ = 0.1–0.6 V vs Ag/AgCl reference electrode). Throughout the experiment period the sample was held potentiostatically at a predetermined constant potential. Impingement experiments were performed by loading approximately 30 zirconia spheres into the main channel, using a hypodermic needle. Subsequent to particles loading, the system was sealed and the experiment was initiated. Figure 3a presents an excerpt of current transient obtained from such an experiment, indicating a single impact. However, in some of the experiments, more than one impact was recorded during the experiment period. Figure 3a presents a single current decay, observed in the transient, resulting from the impact of a single particle at the copper electrode surface in 4 g/L K_2CO_3 solution containing 1 g/L Na_2SO_4 at a potential of 0.2 $V_{Ag/AgCl}$. Initial characterization of the recorded current transient is possible by evaluating its key parameters, such as the peak current I_{max}, the time of peak current t_0, the current rise time t_{rise}, the repassivation time t_{repass}, and the background current I_{back}.

The time axis was normalized to the time of peak current t_0. The peak current in this experiment was recorded to be 0.78 μA. The acceleration of the electrochemical reaction rate produced by particle abrasion of the μ-electrode is a direct consequence of the damage caused to the existing surface oxide films. The rise time of the current increase, recorded after the impact, is only 9 μs before the current reaches its maximum value. The current then decreases to its initial background level within some 740 μs (0.74 ms). The transient shows an exponential decay, typical for a self-inhibiting process such as repassivation.

Subsequent to the impingement process, the copper microelectrode was removed from the slurryjet system, thoroughly rinsed with water, dried, and investigated further with the use of scanning electron microscopy (SEM) and atomic force microscopy (AFM). A microscopic view of the impact crater is shown in Fig. 4a. The diameter and depth of the impact crater are approximately 13.5 and 0.35 μm, respectively (evaluated by AFM line scan). The corresponding sphere radius calculated from the crater dimensions is ~130 μm, in good agreement with the 125 μm zirconia particle diameter. Inside the crater (see Fig. 4a and c) a clear, fine structure with a nanometric feature size can be seen. The size and appearance of these nanoscopic indents obviously fits the nanoscopic substructure of the impacting particles, as seen in Fig. 4b. The highest particle surface feature would correlate to the deepest nanoscopic impact shown in Fig. 4a. The overall shape of the sphere is being imaged in the crater, seen in Fig. 4a. The fact that the crater shown in Fig. 4a has a round shape and no significant scratches caused by the nanoscopic protrusions indicates that the spheres impulse is transferred to the electrode immediately and the sphere most likely loses its whole energy. Removal of the particle from the sample surface is probably caused by the electrolyte jet.

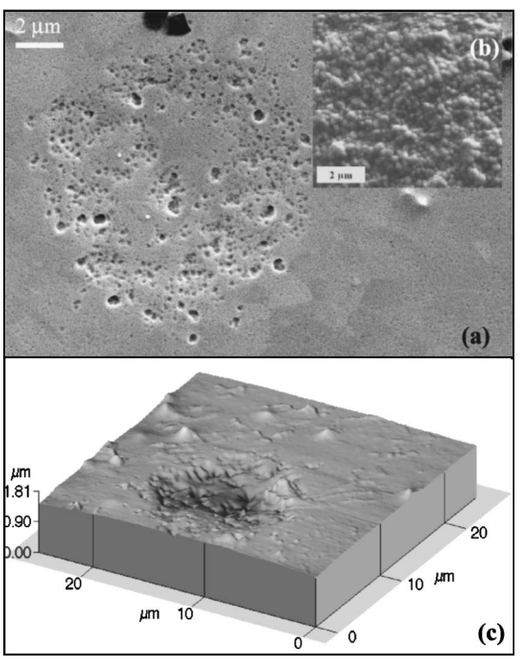

Figure 4. (a) SEM micrograph of the crater obtained subsequent to an impingement in a 4 g/L K_2CO_3 solution containing 1 g/L Na_2SO_4 solution at 0.2 $V_{Ag/AgCl}$. (b) SEM micrographs of ZrO_2 abrasive particle surface. (c) AFM micrograph of the crater.

In order to obtain some statistical values, at each applied potential more than 20 impacts were measured, recorded, processed, and summarized. Impacts having repassivation times 2 orders of magnitude smaller than the time between two close impingements were considered in the statistical calculations. Figures 5a and b present changes in t_{repass} and I_{max}, respectively, obtained from copper impingement in a 4 g/L K_2CO_3 solution containing 1 g/L Na_2SO_4 as a function of the applied potential. The values of t_{repass} do not change significantly as the potential is being raised. The values of t_{repass} at a potential of 200 $mV_{Ag/AgCl}$ were 1.27 ± 0.18 ms (Fig. 5a). At higher applied potentials (200 and 300 $mV_{Ag/AgCl}$) the values of t_{repass} were not changed significantly. The values of t_{repass} were increased by 20% (1.6 ± 0.3 ms) at applied potentials above 300 $mV_{Ag/AgCl}$,while at a potential of 600 $mV_{Ag/AgCl}$ a decrease of 10% in t_{repass} is observed.

The values of I_{max}, recorded during the impact, were relatively high, near 1 μA. These high values are well correlated with the

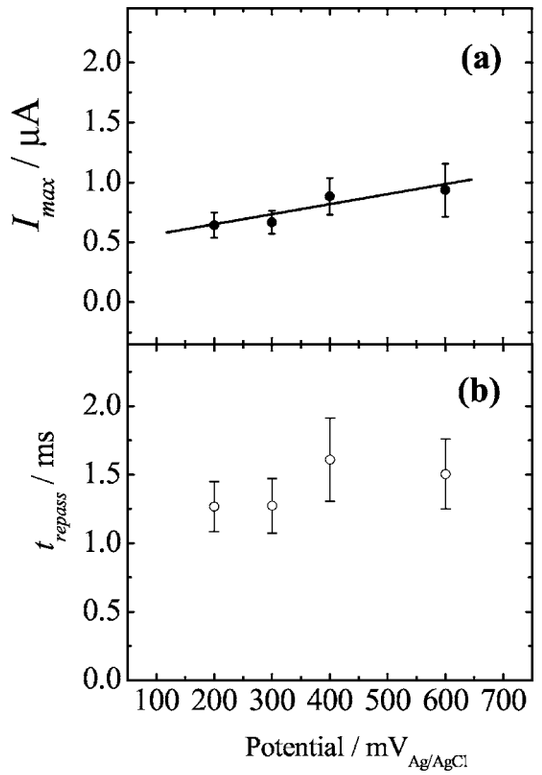

Figure 5. Analysis of electrochemical data during abrasive impingement: (a) current peak (I_{max}) and (b) repassivation time (t_{repass}) at different applied potentials in a 4 g/L K_2CO_3 solution containing 1 g/L Na_2SO_4.

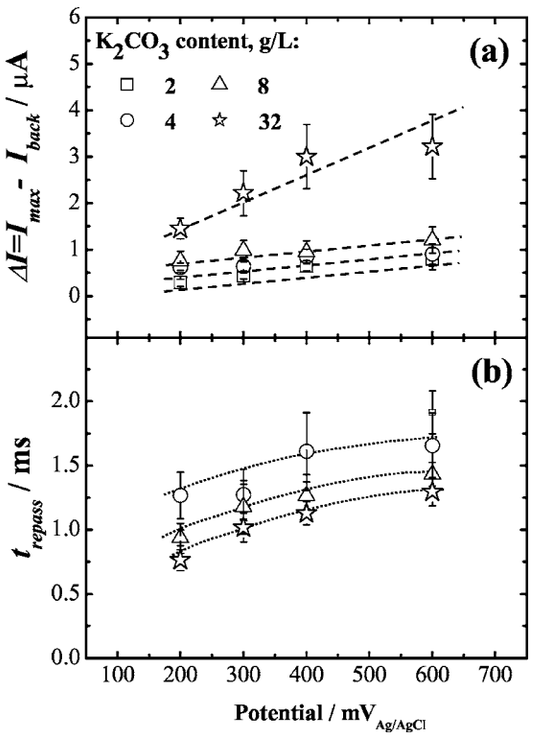

Figure 6. Analysis of electrochemical data during abrasive impingement: (a) current peak (I_{max}) and (b) repassivation time (t_{repass}) at different applied potentials in solutions containing 1 g/L Na_2SO_4 and different K_2CO_3 concentrations.

current values (8.15 mA/cm^2, Fig. 2) obtained from polarizing copper in a pH-adjusted carbonate-free solution containing sulfate ions (taking into account the surface area of the microelectrode being $S_{\mu\text{-electrode}} \cong 1.23 \times 10^{-4}$ cm^2). These current values are dependent on the applied potential: in a 4 g/L K_2CO_3 solution containing 1 g/L Na_2SO_4 I_{max}, values at a potential of 200 $mV_{Ag/AgCl}$ were 0.64 ± 0.104 μA, while at higher applied potentials the I_{max} values increased. Moreover, I_{max} values are linearly dependent on the applied potential imposed on the copper electrode. The linear dependence of I_{max}values on the applied potential can be explained by the contribution of the system's ohmic resistance.

Figures 6a and b present the impact of carbonate (K_2CO_3) content in the solution on the I_{max} and t_{repass} values. Because the current background is different, due to the use of different carbonate solutions, we defined a new parameter which presents the change in I_{max}. This value is represented in Fig. 6a as ΔI, being equivalent to I_{max}–I_{back}. As one can see, an increase in the CO_3^{2-} concentration causes an increase in ΔI values, in the range of the potentials studied. Increasing the carbonate ion concentration from 2 to 8 g/L causes a minor change in ΔI values, while the addition of 32 g/L carbonate ions leads to a significant increase in the current values. Similarly, the slopes of ΔI vs applied potential curves were identical for 1 g/L Na_2SO_4 solutions containing 2, 4, and 8 g/L K_2CO_3, while the use of a solution containing 32 g/L K_2CO_3 provides a much larger slope. The increase in the ΔI values can be explained by the rise in the solution's conductivity. The conductivity and pH values of 1 g/L Na_2SO_4 solutions containing different carbonate ion concentrations is presented in Table I. As one can see, a higher carbonate concentration leads to an increase in the conductivity values and thus a decrease in the solution's ohmic resistance, yielding the observed increase in ΔI values. However, an increase in the CO_3^{2-} concentration has the opposite effect on the values of the copper repassivation time (t_{repass}, Fig. 6b). The increase in carbonate content causes a decrease in the repassivation time values. Values of the repassivation time obtained from 2 and 4 g/L K_2CO_3 solutions are very similar, between 1.27 ± 0.18 and 1.65 ± 0.25 ms, (this value depends on the potential applied). Values of copper t_{repass} in solutions containing higher carbonate concentrations (8 and 32 g/L K_2CO_3) were significantly lower, by approximately 50%, compared with solutions containing lower carbonate concentrations. The decrease in the copper repassivation time in highly concentrated carbonate solutions is most probably related to the formation of copper carbonate species at the copper surface at potentials above 0.1 V_{SCE}. The formation of copper carbonate species at the copper electrode surface in carbonate-based solutions was already reported.[20,30,33] The formation of copper carbonate species at the copper electrodes at potentials above 0.2 V was also confirmed by X-ray photoelectron spectroscopy (XPS) studies.[37] Thus, it is proposed that copper, being polarized in carbonate solutions, would develop an enhanced protective carbonate film.

Effect of impingement angle.— The influence of the impingement angle on I_{max} and the repassivation time (t_{repass}) values of copper in carbonate solutions was also investigated. In order to con-

Table I. Physical and chemical properties of aqueous carbonate solutions.

1 g/L Na_2SO_4 solution containing	Conductivity (mS)	R_{sol} (Ω cm^{-2})	pH
2 g/L K_2CO_3	5	115.3	11.2
4 g/L K_2CO_3	7.8	96.7	11.3
8 g/L K_2CO_3	13.6	47.1	11.5
32 g/L K_2CO_3	43.5	15.56	11.7

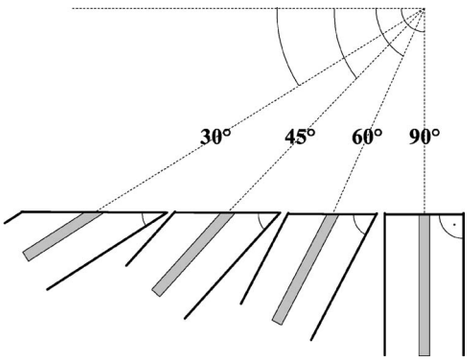

Figure 7. Schematic presentation of copper electrode sample prepared at different impingement angles.

duct such experiments the μ-electrodes were mechanically polished at different angels. Figure 7 presents a schematic view of copper μ-electrodes polished at 90, 60, 45, and 30°. Grinding and polishing the samples at different angles leads to an increase in the electrode surface area. The surface areas were increased (compared to a 90° grinding angle) by 15, 41, and 100% at angles of 60, 45, and 30°, respectively.[36]

Figure 8 shows the recorded transients and the analogue SEM micrographs, side by side, presenting both the current decays and the morphology (SEM) developed on the copper surfaces subsequent to the impingement. The craters formed, resulting from a single impact at the impingement angles of 90, 60, 45, and 30°, are shown. All the impingements were conducted on copper μ-electrodes in a 4 g/L K_2CO_3 solution containing 1 g/L Na_2SO_4 at a potential of 0.2 $V_{Ag/AgCl}$. Reducing the impingement angle from

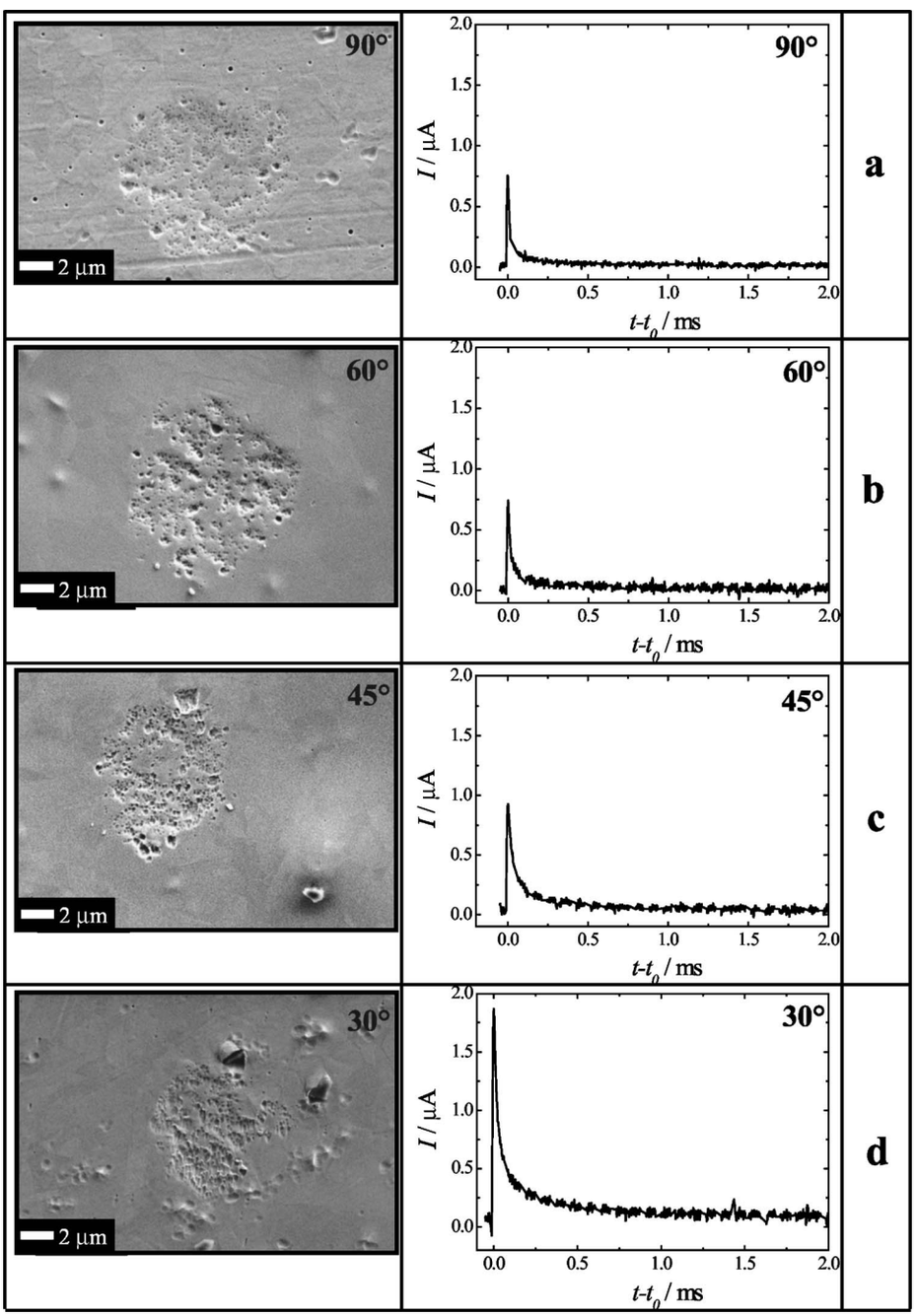

Figure 8. Repassivation transients with the corresponding SEM micrographs presenting the impact craters obtained subsequent to impingements at different angles: (a) 90, (b) 60, (c) 45, and (d) 30°. All impingement studies were performed in a 4 g/L K_2CO_3 solution containing 1 g/L Na_2SO_4 at a potential of 0.2 $V_{Ag/AgCl}$.

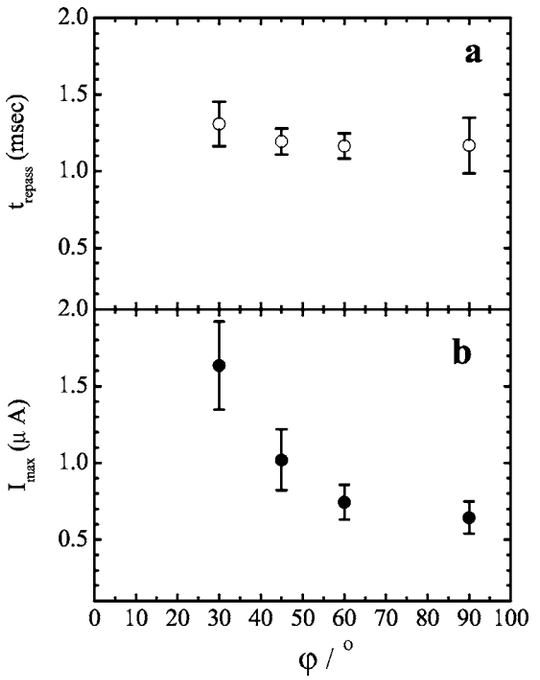

Figure 9. Analysis of electrochemical data during abrasive impingement at different angles: (a) repassivation time (t_{repass}) and (b) current peak (I_{max}) in a solution containing 1 g/L Na_2SO_4 and 4 g/L K_2CO_3 at a potential of 0.2 $V_{Ag/AgCl}$.

90 to 30° results in a modification of the impact crater, from an almost perfectly round circle (Fig. 8a) towards an elongated (oval) feature with a smaller diameter (Fig. 8d). In addition, the formation of nanoscopic indents at the copper surface at an impact angle of 90° (Fig. 8a) was observed. As the angle decreases (from 90 to 30°) an additional feature transformation of the indents was observed, from singular nanoindents with an average diameter of 100 nm (Fig. 8a and b) towards sliding grooves with lengths of 300 nm (Fig. 8c) and 1 μm (Fig. 8d) at impingement angles of 45 and 30°, respectively, and a width of 100 nm. This "scratching" is a result of the nanoroughness of the ZrO_2 particles (Fig. 4b).

Figure 9 presents the influence of different impingement angles on the repassivation time (t_{repass}, Fig. 8a) and peak current (I_{max}, Fig. 8b) in a 4 g/L K_2CO_3 solution containing 1 g/L Na_2SO_4 at an applied potential of 0.2 $V_{Ag/AgCl}$. Copper repassivation time at an impingement angle of 90° was recorded to be 1.17 ± 0.18 ms. At lower impingement angles of 45 and 30° no significant changes in repassivation time were recorded (1.2 ± 0.085 and 1.3 ± 0.145 ms, respectively). Moreover, the current rise time (t_{rise}, Fig. 3b) subsequent to the impacts was 12 μs for all impingement angles (90, 60, 45, and 30°). However, the peak current (I_{max}) values gradually increase as the impingement angles decrease.

Inspecting the current peak values shows that a reduction in the impingement angle causes a gradual and steady increase in the current peak values, as shown in Fig. 9b. Peak currents obtained from impingement angles of 90 and 60° were 0.64 ± 0.1 and 0.74 ± 0.1 μA, respectively. At a lower impingement angle (45°) the peak current value increased slightly to 1.02 ± 0.2 μA, while at an impingement angle of 30° the peak current value was significantly higher at 1.65 ± 0.3 μA. Background current was higher at a 30° angle than at higher impingement angles, because the exposed sample area was increased. However, this effect cannot explain the significant increase in the peak current values. It was shown by Akiyama et al.[36] that the crater is not completely depassivated on impact; rather, the oxide is cracked and/or pierced by the impacting particle. At lower angles, scratching contributes an additional component to the total amount of wear. The amount of scratching is dependent on the impact angle; upon perpendicular impingement the impacting particle rebounds from the sample surface, leaving a round impact crater. At an angle of 60° the amount of scratching is very low; the largest grooves were obtained after impingement at an angle of 30°. At very low impingement angles the crater size was reduced, showing a larger scratching effect. It is assumed that the increase in the peak current values is due to the sliding effect, causing the formation of extended scratch marks. Our studies show that altering the impingement angle does not have any significant effect on the repassivation and depassivation (t_{rise}) time. This would mean that it is the carbonate which rapidly develops enhanced passivity without any correlation to the exposed copper surface area.

Conclusions

Copper develops an extended passivity range in sulfate solutions containing potassium carbonate. The addition of low carbonate concentration, namely 4 g/L potassium carbonate, to a 1 g/L sodium sulfate solution provides an extended passivity range. This enhanced copper passivity is highly stable even at potentials above 1 $V_{Ag/AgCl}$.

The depassivation and passivation characteristics of the protective layers formed at the copper surface in carbonate-based solutions in the potential region from OCP up to 0.6 $V_{Ag/AgCl}$ were studied by the use of a slurryjet instrument. It was shown that the repassivation rate of copper electrodes in carbonate-based solutions in a wide potential range was between 1.2 ± 0.18 and 1.6 ± 0.3 ms. I_{max} values were recorded to be near 1 μA, with a linear dependence on the applied potential.

An increase in carbonate concentration leads to an increase in the I_{max} values, especially in solutions with carbonate concentrations of 32 g/L. An increase in carbonate ion concentration from 2 to 8 g/L does not lead to changes in I_{max} values, while the addition of 32 g/L of carbonate ions causes a significant increase of the current values. The increase in I_{max} values is due to the increase in the solution's conductivity. However, an increase in carbonate content leads to a decrease in repassivation time values. The decrease in copper repassivation time in highly concentrated carbonate solutions is mainly attributed to the formation of protective copper carbonate species at the copper surface at potentials above 0.2 $V_{Ag/AgCl}$.

The influence of the impingement angle on the peak current, the repassivation time, and the depassivation time of copper in carbonate solutions was investigated and it was found that depassivation and repassivation times were not affected by abrasive impingement angle, while the values of peak current increased as the impingement angle decreased. The observed increase in the current peak values is due to the formation of sliding grooves which enhance metal surface wear.

Thus, the use of a carbonate anion as a passivating component in a future CMP slurry design should be considered, because the main requirement (high rate of repassivation) is being fulfilled in carbonate-based solutions.

Acknowledgments

This work was supported by a Minerva Travel Grant of the Max-Planck Society, which funded E.A.'s travel to and research at the Max-Planck-Institut für Eisenforschung in Düsseldorf. This research was also supported by the R. Biss Metallurgy Research Fund of the Technion-Israel Institute of Technology.

Technion-Israel Institute of Technology assisted in meeting the publication costs of this article.

References

1. J. M. Steigerwald, S. P. Murarka, and R. J. Gutmann, *Chemical Mechanical Planarization of Microelectronic Materials*, Wiley, New York (1997).
2. S. Lakshminarayanan, J. Steigerwald, D. T. Price, M. Bourgeois, T. P. Chow, R. J. Gutmann, and S. P. Murarka, *IEEE Electron Device Lett.*, **15**, 307 (1994).
3. M. B. Small and D. J. Pearson, *IBM J. Res. Dev.*, **34**, 858 (1990).
4. P. Singer, *Semicond. Int.*, **21**, 90 (1998).
5. R. Lui, *Solid-State Electron.*, **43**, 1003 (1999).

6. Y. Ein-Eli, E. Abelev, E. Rabkin, and D. Starosvetsky, *J. Electrochem. Soc.*, **150**, C646 (2003).
7. E. Paul, F. Kaufman, V. Brusic, J. Zhang, F. Sun, and R. Vacassy, *J. Electrochem. Soc.*, **152**, G322 (2005).
8. Z. Li, K. Ina, P. Lefevre, I. Koshiyama, and A. Philipossian, *J. Electrochem. Soc.*, **152**, G299 (2005).
9. Y. Ein-Eli, E. Abelev, and D. Starosvetsky, *Electrochim. Acta*, **49**, 1499 (2004).
10. R. K. Singh, S. M. Lee, K. S. Choi, G. B. Basim, W. Choi, Z. Chen, and B. M. Moudgil, *MRS Bull.*, **27**, 752 (2002).
11. S. Aksu, L. Wang, and F. M. Doyle, *J. Electrochem. Soc.*, **150**, G718 (2003).
12. Y. Ein-Eli, E. Abelev, and D. Starosvetsky, *J. Electrochem. Soc.*, **151**, G236 (2004).
13. G. B. Shinn, V. Korthuis, and A. M. Wilson, *Handbook of Semiconductor Manufacturing Technology*, p. 415, Marcel Dekker, New York (2000).
14. F. B. Kaufman, D. B. Thompson, and R. E. Broadie, *J. Electrochem. Soc.*, **138**, 3460 (1991).
15. M. Pourbaix, *Atlas of Electrochemical Equilibria in Aqueous Solutions*, 2nd ed., NACE, Houston, TX (1974).
16. V. Maurice, H. H. Strehblow, and P. Marcus, *Surf. Sci.*, **458**, 185 (2000).
17. S. M. Wilhelm, Y. Tanizawa, C. Liu, and N. Hackerman, *Corros. Sci.*, **22**, 791 (1982).
18. D. D. Macdonald, *J. Electrochem. Soc.*, **121**, 208 (1966).
19. W. Kautek and J. G. Gordon, *J. Electrochem. Soc.*, **137**, 2672 (1990).
20. H. H. Strehblow and B. Titze, *Electrochim. Acta*, **25**, 839 (1980).
21. D. Tromans and R. Sun, *J. Electrochem. Soc.*, **139**, 1945 (1992).
22. H. Y. H. Chan, C. G. Takoudis, and M. J. Weaver, *J. Phys. Chem. B*, **103**, 357 (1999).
23. R. L. Deutscher and R. Woods, *J. Appl. Electrochem.*, **16**, 413 (1986).
24. J. Ambrose, R. J. Barradas, and D. W. Shoesmith, *J. Electroanal. Chem. Interfacial Electrochem.*, **47**, 47 (1973).
25. J. Ambrose, R. J. Barradas, and D. W. Shoesmith, *J. Electroanal. Chem. Interfacial Electrochem.*, **47**, 65 (1973).
26. J. W. Schultze and A. W. Hassel, in *Encyclopedia of Electrochemistry*, A. J. Bard and M. Stratmann, Vol. 4, *Corrosion and Oxide Films*, M. Stratmann and G. S. Frankel, Volume Editors, pp. S. 216–270; *Encyclopedia of Electrochemistry*, A. J. Bard and M. Stratmann, Vol. 4, *Corrosion and Oxide Films*, M. Stratmann and G. S. Frankel, Volume Editors, 188–189, Wiley-VCH Weinheim (2003).
27. I. T. E. Fonseca, A. C. S. Marin, and A. C. Sa, *Electrochim. Acta*, **37**, 2541 (1993).
28. T. Hurlen, G. Ottesen, and A. Staurset, *Electrochim. Acta*, **23**, 39 (1978).
29. I. Milošev, M. Metikos-Hukovic, M. Drogowska, H. Menard, and L. Brossard, *J. Electrochem. Soc.*, **139**, 2409 (1992).
30. R. M. Souto, S. Gonzalez, R. C. Salvarezza, and A. J. Arvia, *Electrochim. Acta*, **39**, 2619 (1994).
31. Y. Ein-Eli, E. Abelev, M. Auinat, and D. Starosvetsky, *Electrochem. Solid-State Lett.*, **8**, B69 (2005).
32. M. Perez-Sanchez, R. M. Souto, M. Barrera, S. Gonzalez, R. C. Salvarezza, and A. J. Arvia, *Electrochim. Acta*, **38**, 703 (1993).
33. E. Mattsson and A. M. Fredriksson, *Br. Corros. J., London*, **3**, 246 (1968).
34. J. N. Thomas and A. K. Tiller, *Br. Corros. J., London*, **7**, 257 (1972).
35. A. W. Hassel and A. J. Smith, *Corros. Sci.*, In press.
36. E. Akiyama, A. W. Hassel, and M. Stratmann, *J. Phys. D*, Accepted for publication.
37. Y. Ein-Eli and E. Abelev, Unpublished results.